Influência da fendilhação na durabilidade de betão reforçado com nanotubos de carbono

Influence of cracks on the durability of reinforced concrete with carbon nanotubes

Tomás Azevedo Mendes Fernandes Diniz

Resumo alargado

Extended Abstract

Orientadores:

Professor Doutor José Alexandre de Brito Aleixo Bogas

Doutora Hawreen Hasan Ahmed

Júri:

Presidente: Professor Doutor Jorge Manuel Caliço Lopes de Brito

Orientador: Professor Doutor José Alexandre de Brito Aleixo Bogas

Vogal: Professor Doutor Pedro Miguel Soares Raposeiro da Silva

Setembro 2020

Influence of Cracks on the Durability of reinforced concrete with Carbon Nanotubes

Tomás Diniz

Master's in Civil Engineering

Instituto Superior Técnico, Universidade de Lisboa, Portugal, 2020

Keywords: Reinforced concrete with carbon nanotubes; Artificial Cracking; Natural Cracking Capillary absorption; Carbonation resistance; Chloride penetration.

1. Introduction

Concrete is a quasi-brittle material that is highly susceptible to the appearance of cracks during its designed service life. Cracks in concrete can appear for different reasons. On the one hand, mechanical actions and poor designing can induce structural cracks. On the other hand, hygrothermal variations, restrained shrinkage and concrete deterioration mechanisms, such as freezing and thawing and other expansive reactions (reinforcement corrosion, alkali-silica reaction) can lead to nonstructural cracks. When the local tensile stresses in concrete exceed its maximum tensile strength, cracks are formed, and new external and internal paths are established. These new paths should increase concrete permeability and may favor the penetration of deleterious species, inevitably affecting its durability.

The high use of concrete led to various efforts in the search and development of this material. As an answer to the rising demand and structural challenges, the application of reinforced fibers, in the concrete matrix, aims to improve the concrete ductility and control over cracks, during its creation and opening stages. However, the usual fibers are unable to act at a micro level, preventing this small crack to become larger and turn into macrocracks.

Carbon nanotubes (CNTs) were recently discovered, in the past decade they have been extensively studied as a reinforcement material for cement-based composites. The growing interest in this field comes from the desire to modify the cement matrix at the scale of their main compounds. Taking advantage of the outstanding properties of CNTs. On the one hand, CNTs have ultra-high strength and stiffness, with Young's modulus up to 1 TPa and exceptional tensile strength upt to 100 GPa [1]. On the other hand, they have extremely high aspect ratios (1:1000) and surface area (up to 1000 m^2/g), as well as very low density (1500 kg/m^3). Therefore, CNTs are ideal candidates for cement nano-reinforcement, being potentially able to retain the propagation of small nano-cracks and improving some negative features of cement-based materials, such as the low tensile strength and low strain capacity. In fact, CNTs have proven to enhance the fracture properties and early age strain capacity of cement pastes and mortars, reducing or preventing crack initiation [2],[3].

Due to their significant capillary forces, pore sizes has a great impact in the concrete shrinkage, creep, permeability, strength cement hydration [4],[5]. CNTs, due to its small dimension, are able to affect the concrete porous structure and can work as fillers, reducing the number of pores below 50 nm [6]. The source of shrinkage and creep is provided by the hydrated cement paste. Therefore, the incorporation of CNTs in concrete is expected to essentially affect the source of time-dependent shrinkage and creep, by densifying the cement paste microstructure (nucleation and filler effect) and by controlling the propagation and development of microcracks (bridging effect).

So far, only a few works have been published concerning the characterization of reinforced concretes with CNTs. Some results are inconsistent and are mainly focused in cement pastes and mortars. There's a consensus that CNT's can clearly improve cement mixtures, however, the main obstacle is still to reach high levels of dispersion in the composition.

Table 2 - Concrete compositions

Compositions	w/c	Cement (kg/m³)	Water (kg/m³)	Fine sand (kg/m³)	Coarse sand (kg/m³)	Fine gravel (kg/m³)	Coarse gravel (kg/m³)	CNT (g/m³)
BR	0,55	380	214	303	454	242	710	
BCNTs		380	210	303	454	242	710	4222

2. Experimental campaign

I. Materials

One type of industrial multi-walled carbon nanotubes was selected to produce the reinforced mixture (CNTSS). Supplied by timesnano, these CNTs were already in aqueous suspension, named TNWPM-M8. Nevertheless, it was necessary to disperse them in a more fluid suspension. Their main properties are listed in Table 1. For concrete production, cement type I 42.5 R according to EN 197-1, two crushed limestone coarse aggregates with D_{max} of 10 mm and two natural siliceous sands were selected.

Table 1 – CNT properties

Purity	Di*	De*	lenght	ASE*	Fresh density
>98%	5-15 nm	20-80 nm	<10um	>60 m2/g	~2.1 g/cm3
Di – Inner diametre; De – Outer diameter; ASE – Special surface area					

II. Dipersion of multi-walled CNTs

The Multi-walled CNTs used were dispersed by a physical procedure, involving first a sonication and later a magnetic stirring off the aqueous suspension. The dispersion process was selected according to a previous research [7]. The type of CNTs used (CNTSS) were already supplied in aqueous suspension, previously stabilized by the manufacture, using a polyethylene-based dispersant. The procedure involved a 45 minutes sonication followed by magnetic stirring, with 40% of the mixing water, for at least 1 hour.

III. Concrete mixing

To analyze the efficiency of the CNTs two concrete mixes were produced, with the same w/c of 0,55. One mixture reinforced with CNTs and a normal one, without CNTs, for comparison purposes. The compositions are presented in Table 2. The optimal amount of CNTs, by weigh of cement (%wtc), was determined considering the results of mechanical characterization of cement pastes with 0.015–0.1%wtc of the same type of CNTs used in this study: 0.1%wtc for CNTSS was determined for mixtures. According to the literature [8],[9].

Concretes were produced in a vertical shaft mixer with bottom discharge. The CNTs dispersion was first prepared. The mixing procedure began with the incorporation of all the aggregates in the mixer in descending order of its size and mixed for 1 min. The mixer was not stopped and 60% of the total mixing water was added. The mixing kept for another 3 min. After this stage the mixer was stopped for 1 min. The cement and remaining water, with CNTs when in use, were then added to the mixer for another 4 min of mixing. In total, the mixing procedure lasted approximately 8 min. After mixing, the slump was measured according to EN 12350-2 [10].

The following specimens were produced for each mix: four 150 mm cubic specimens for compressive strength tests at 28 days according to EN 12390-3 [11]; nine Φ10x20 cylindrical specimens for testing capillary absorption, carbonation and chloride penetration in uncracked and artificially cracked specimens; six 60x15x15 prisms to produce the 18 natural cracked specimens needed for the capillary absorption, carbonation and chloride penetration test.

IV. Curing

All specimens were demolded after 24 hours and kept in a wet chamber for 7 days. After this, different curing steps were followed. The cubic specimens, for the compressive strength test, and the cylindric ones, for the chloride penetration, were kept in the same wet chamber until testing. To test capillary absorption specimens were pre-conditioned according to LNEC E393: after those 7 days the samples were sawn into smaller specimens, which were kept in a controlled chamber (T=22 ± 2 °C; RH=50 ± 5%) for 7 days. Then, they were oven dried at 60 ºC for 3 days. The specimens were then covered with a plastic tape and kept in the same oven for 10 days. The specimens for carbonation were pre-conditioned according to LNEC E391 [12], being water cured for 7 more days and then placed in the dry chamber until testing. All specimens were left at ambient temperature for one day before testing.

V. Pre-cracking concrete

There are two distinct types of cracks that can be induced in concrete specimens: artificial and natural cracks. Each one has strong and weak points. Artificial cracks have uniform characteristics, with control over the crack width and are easier to replicate. Natural cracks are better to simulate reality, with tortuous and non-uniform geometry, but the crack width and repeatability are challenging to control.

Artificial cracks were obtained using the notch method, in which a thin plate with a 0.05mm thickness was inserted in the sample, while the concrete was still fresh (Fig. 1). This method allows for a good control of the crack since it is easier to simulate the intended crack width accurately. After a few hours, when the concrete had some consistence, the plates were removed leaving a crack with the desire width. Based on previous studies [13] to ensure that the plates were easily removed, it was determined, for concretes with w/c of 0.55, that the plates should be removed from the specimens after 5 hours. In this study, to obtain the desired width of 0.05mm and get a final crack depth of about 10mm., plastic plates were inserted 20mm deep into the concrete. The main disadvantage of this method is that the metallic plate induces wall-effect and smooth cracked surface, which deviates from the real behavior of cracked concrete.

Fig. 1 – Artificial crack

Natural cracks were obtained on beams specimens with 60x15x15cm, with a three point controlled bending method. To prevent the sudden failure of the beam and control the crack width, beams were reinforced with two Φ6 A500NR steel bars at the bottom. Two different widths of natural cracks were studied, 0.05 and 0.1mm. For each composition six beams were produced, three with 0.05mm cracks and three with 0.1mm cracks.

A hydraulic INSTRON press with 250 KN load capacity was adopted. In each pre-cracked section, the crack width was controlled with linear variable differential transformer (LVDT) from TML, model CDP-25 with a 25mm stroke placed on both sides of the sample (Fig. 2). The values of stress and strain were registered using an HBM Spider8 data logger. Various loading and unloading cycles were carried out to obtain the desired crack width after unloading. Three cores with Φ 9.5×15 (cm) were drilled from the cracked zones of each beam using a HILTI core drill. Each core was then wrapped with a tight tape and sectioned into Φ 9.5×5 (cm) samples destined for testing. Due to the inherent difficulty of controlling this method, the final crack width was on average higher than wanted. 0.03-0.1 mm to desire cracks of 0.05 mm and 0.1-0.2 mm to desire cracks of 0.1mm. This was measured using a electronic microscope with image treatment.

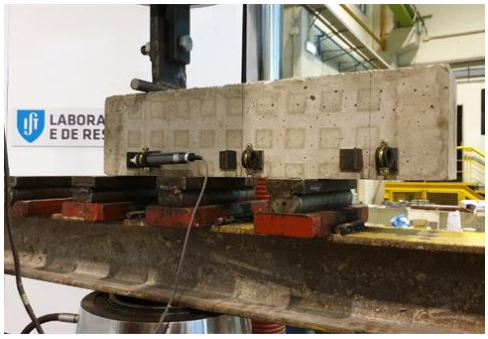

Fig. 2 – Natural cracking

VI. Capillary absorption

Capillary absorption was determined at 28 days in compliance with,LNEC E393 [14]. The test consists in measuring the water uptake of the specimen by measuring the mass increase due to water absorption as a function of time when one surface of the specimen is immersed in a 5 ± 1mm film of water. The mass of the specimen was recorded at 10,20, 30 min and 1, 3, 6, 24 and 72 h, after initial contact with water. From the absorption curve plotted against the square root of time, different coefficients of absorption were determined as equivalent to the slope of the linear regression line. For each composition, three reference uncracked specimens, three specimens with artificial cracks of 0.05mm width, three specimens with 0.05mm natural cracks and three specimens with 0.1mm natural cracks were tested.

VII. Carbonation resistance

The accelerated carbonation test was carried out according to LNEC E391 [12]. Specimens with artificial and natural cracks were tested. However, due to the differences between cracking methods, different techniques were used during the test. After curing, the artificial cracked specimens (Φ 10×5 cm) were painted in all surfaces except the cracked one. Which allows the control of the carbonation flow through the specimen. Then they were placed in a carbonation chamber at 23 ± 3 _C, 60 ± 5% RH, 5 ± 0.1% CO_2 and taken out at 28, 56 and 90 days. The natural cracked specimens were covered with tape

around the lateral and in the bottom. The top surface, with the crack, was left unprotected. After this they were placed in the same carbonation chamber and tested at 7 and 28 days. The specimens were sectioned longitudinally, crossing the length of the crack perpendicularly. The specimens were then air dried for 24 h and placed back in the carbonation chamber. One cut was done at each testing age, as exemplified in Fig. 3

Fig. 3 – Natural cracked specimens sectioned

The carbonation depth was measured after spraying a phenolphthalein solution on the freshly broken surfaces. In cracked specimens two different measures were taken, one in the cracked area and another in the uncracked one (Fig. 4). Phenolphthalein reacts with the alkaline components of cement, turning pink in areas where pH is above 9. One specimen for each combination of composition and crack width was tested per age. The carbonation coefficient, K_c, was obtained from the linear regression between carbonation depth, Xc, and the square root of time, $t^{1/2}$, by applying Fick's first law of diffusion through Eq. (1).

$$x_c = K_c t^{1/2} \quad [mm/ano^{1/2}] \qquad (1)$$

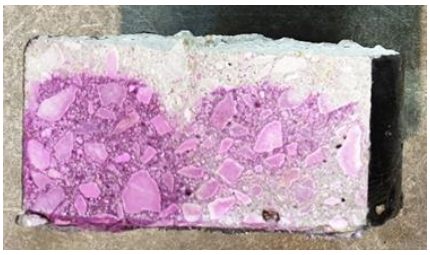

Fig. 4 - Reaction of the phenolphthalein in specimens subject to carbonation test

VIII. Chloride penetration resistance

The chloride penetration resistance was determined by the rapid chloride migration (RCM) test, according to LNEC E463 and NTbuild492 [15], which provides a chloride ion migration diffusion coefficient (D_{CL}) under non-steady conditions. Three Φ10×5 cm cylindrical specimens were tested per each concrete composition. An external electrical potential was applied to force migration of chloride ions into the specimen, which was then split in two and sprayed with a silver nitrate solution. The chloride penetration depth corresponds to the limit of the white silver chloride precipitation. Seven measures were taken in each exposed face. The diffusion coefficient was calculated according to Eq. (2), where T represents the average value of the initial and final temperature of the anodic solution (ºC), L is the specimen's thickness (mm), U is the absolute value of the applied voltage (V), t is the test duration (hours) and x_d is the average value of the measured chloride penetration depth (mm).

$$D_{cl} = \frac{0{,}0239(273+T)^L}{(U-2)^t}\left(x_d - 0{,}0238\sqrt{\frac{(273+T)Lx_d}{U-2}}\right) \quad [\times 10^{-1} m^2/2] \qquad (2)$$

3. Results and discussion

I. Fresh-estate properties, concrete density and compressive strength

The average slump, fresh density (ρ_f), dry density (ρ_d) and compressive strength (fcm,28d) are presented in Table 3. Due to the small percentage of CNTs used in the reinforced mixture, 0.1% of cement past, test results show that there was not much difference between the workability of the two mixes. It has been reported that incorporation of CNTs tends to decrease the workability of cement pastes [16][17], due to the large CNTs surface area which promotes significant surface interactions with the mix. However, the slump test led to slightly higher results in the reinforced mixture, the use of low dosages of CNTs didn't significantly alter the slump. Similar behaviour was reported by Collins et al. [18] and Konsta et al. [19] in cement pastes, attributed to the good dispersion of CNTs and high effectiveness of the dispersant.

Table 3 – Compressive streght, fresh and dry density

Mix	Cement	w/c	ρ_f (kg/m³)	Δ(%)	Slump (cm)	ρ_d (kg/m³)	Δ(%)	$f_{cm,28d}$ (MPa)	Δ(%)
BR	CEM I 42,5	0,55	2290	-	17,5	2354	-	45,6	-
BCNTs			2303	0,6	18,0	2364	0,4	50	9,8

The dry density results show that, as in the slump test and fresh density, differences between mixes were not significant. It may be concluded that CNT-reinforced concrete shows a similar behaviour to reference concrete.

Compressive strength tests confirmed a difference between reinforced and reference concrete. It was a small upgrade, but the mixture with CNTs, showed a 10% improvement during the test. Other authors [20] reported slightly higher results with the same type of CNTs and similar concrete (equal w/c). The difference between these results can be related with a lower quality of the mixture. The level of CNTs dispersion reached in the present study could by lower than wanted. This might happen due to the poor quality of the carbon nanotubes, which were stored for at least 2 years. Nevertheless, the incorporation of CNTs revealed a contribution to the improvement of concrete mechanical resistance. The CNTs mechanisms responsible for this are the filler, nucleation and bridging effect, which are often related to carbon nanotubes.

II. Capillary absorption

The incorporation of CNTs can essentially reduce the capillary absorption of concrete in two ways: by filler and nucleation effects, refining the microstructure of concrete, namely in the paste and at the aggregate-paste ITZ; by bridging effect, contributing to reduction of the formation and propagation of macrocracks, which may increase pore connectivity. In general, all the compositions showed absorption curves with similar shape (Fig. 5). Contrarily to what would be expected, the curves do not vary linearly with the root of time. This is essentially related to the non-uniform moisture distribution in the concrete depth. In fact, absorption curves are characterized by a higher rate of absorption in the first three hours, followed by a significant decrease in the rate of absorption for later periods. Therefore, for uncracked specimens, each phase was analysed separately. Two absorption coefficients were calculated, one for the initial period and another to later one. Both coefficients, as well as the water absorption at 72 hours, are displayed in Table 4. There's a big reduction in the final stage of the test, therefore for each mixture the greater reduction is register between the first coefficient ($C_{abs,\ 0\text{-}3h}$) and the final one ($C_{abs,\ 6\text{-}72h}$). At later stages the smaller pores are already full of water which means that is harder for the water to access the concrete porous structure. The highest difference between reinforced and nonreinforced concrete was register at later stages ($C_{abs,\ 6\text{-}72h}$) with a decrease around 27% for the reinforced mixture. In fact, this was unexpected since CNTs should show a better contribution at early stages, as reported by other authors [13]. These results were difficult to sustain, yet, it could happen due a higher participation of the gel pores and possibly long-term diffusion phenoms. The absorption at 72 hours register a reduction of 12.3% for reinforced concrete. This reduction was lower than the difference between coefficients, meaning that CNTs contributed for the refinement of the porous structure and not that much for the reduction of total porosity.

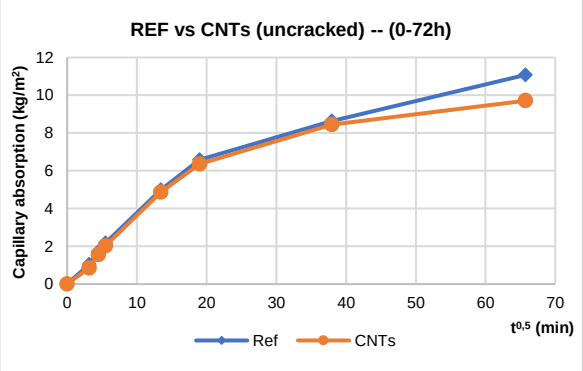

Fig. 5 - Absorption curve for uncracked concrete

Table 4 – Absorption coefficient

Mixture	w/c	$C_{abs,\ 0\text{-}3h}$		$C_{abs,\ 6\text{-}72h}$			Abs_{72h}		K_{IF}
		mm.min$^{0.5}$	Δ(%)	mm.min$^{0.5}$	Δ(%)	R^2	(Kg/m^2)	Δ(%)	
BR	0,55	0,371	-	0,095	-	0,99	11,077	-	0,954
BCNTs		0,363	2,2	0,069	27,4	0,94	9,711	12,3	0,868

Table 5 – Absorption coefficients (artificial cracks)

Mixture	w/c	L_f (mm)	Artificial crack (0,05 mm)	
			$C_{abs}A._{\ 0\text{-}3h}$	$C_{abs}A._{\ 6\text{-}72h}$
			mm.min$^{0.5}$	mm.min$^{0.5}$
BR	0,55	18	0,515	0,132
BCNTs		18	0,466	0,107

In the Table 5 are the absorption coefficients results for the artificial cracked specimens. As expected, the specimens had a higher absorption and therefore higher absorption coefficients, in comparation to the uncracked ones. This is a result of the higher initial

absorption promoted by the crack itself. After this initial effect, the results tend to similar values of the uncracked. However, in the cracked concrete the absorption coefficient should always be higher. The cracked specimens also showed the effect of the CNTs in the reduction of the absorption coefficients. In this case, beyond the filler and nucleation effect, the bridging effect should have a more active role in the reduction of the absorption values, creating bridges around the cracked area making it more difficult for the water to penetrate the concrete porous. The absorption, in artificially cracked specimens is hard to evaluate in the crack area, mainly because of the differences between crack depths. Therefore, to better understand the influence of the crack, following previous studies (8), a crack coefficient was determined (Eq.(3)), which is independent from the crack depth. Abs_{fend} is the absorption in cracked specimens, Abs_{ref} is the absorption in uncracked specimens, A_0 is the surface area, D is the diameter and L_f is the crack lenght. The results are shown in the Table 4 and they show higher values to the reference concrete than to the reinforced one. This demonstrates that the crack had a more relevant impact in the absorption for the reference concrete. Which ultimately means that the CNTs had some impact in the improvement of the concrete structure.

$$K_{IF} = \frac{Abs_{E\,fend} \times A_0}{\frac{A_0 + (2L_f \times D)}{Abs_{E\,ref}}} \qquad [3]$$

The absorption coefficient in the cracked area has to be much higher than in the uncracked area. To better analyse the influence of the crack, a coefficient for the absorption in the crack (Eq. (4)) was determined. This coefficient represents the additional rate of water absorption

due to the crack. The water absorption in the cracked region (abs_{ZF}) is obtained from Eq. (4), where A0, absc and abs_{ref} were defined in Eq. (2) considering that this additional water only penetrates through the cracked area, A_C, which corresponds to the product of the crack width with the diameter of the specimen.

$$C_{abs}A._{ZF} = \frac{Abs_{ZF}}{A_c \times \sqrt{t}} \qquad [4]$$

$$Abs_{ZF} = (Abs_{E\,fend} \times A_0) - Abs_{E\,ref} \times (A_0 - A_f) \qquad [5]$$

Fig. 6 shows the variation of $C_{abs}A._{ZF}$ over time. It is confirmed that the influence of the crack is more significant in the first minutes of the test, exponentially reducing over time. The Table 6 shows the absorption coefficient in the early stages of the test 10,20 and 30 minutes, in the cracked area. Results show that the crack area has significantly higher values than the uncrack area. This allows us to conclude that artificial cracks don't resist to capillary absorption.

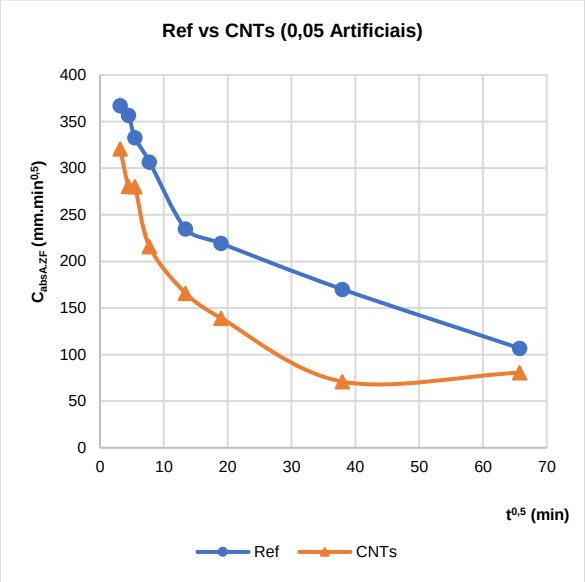

Fig. 6 – Absorption coefficient in the crack area

Table 6 – Values of the absorption coefficient in the crack area

Mix.	w/c	10 min		20 min		30 min	
		$C_{abs}A.$	$C_{abs}A._{ZF}$	$C_{abs}A.$	$C_{abs}A._{ZF}$	$C_{abs}A.$	$C_{abs}A._{ZF}$
Ref.	0,55	0,328	367	0,385	357	0,396	333
CNTs		0,271	321	0,348	281	0,368	280

Specimens with natural cracks are not comparable with any of the above, since the dimensions and geometry are different. In these specimens the crack goes through all the thickness of the specimen, due to the adopted cracking method. Therefore, only the early absorption was considered. The Table 7 has the abortion values at 10,20,30 minutes and 72 hours. The respective coefficients are also shown. Natural cracked specimens were tested with two different crack openings (0.05 and 0.1mm), results show that absorption and respective coefficient tend to be higher in larger cracks. A wider crack creates a rise in the porous structure of the concrete which allows more water to penetrate the material. Carbon nanotubes also worked in this kind of cracked specimens. It's possible to compare two different mixtures and realize that there's an improvement in the absorption coefficient. This improvement (18%) was more noticeable in smaller cracks (0.05mm), where CNTs can work better and the bridging effect should have a higher contribution to control the capillary absorption.

Table 7 – Absorption coefficients (natural crack)

Mix.	w/c	L_f	Natural crack (0,05 mm)						
			Absorption (kg/m²)				Absorption coefficient (mm.min^{0,5})		
			10min	20min	30min	72h	$C_{abs}N._{0\text{-}20min}$	$C_{abs}N._{20\text{-}30min}$	$C_{abs}N._{6\text{-}72h}$
BR	0,55	0,1	1,02	1,12	1,16	2,42	0,264	0,041	0,017
BCNTs		0,08	0,82	0,93	0,97	2,28	0,217	0,041	0,018
Mix.	**w/c**	**L_f**	**Natural crack (0,1 mm)**						
			Absorption (kg/m²)				**Absorption coefficient (mm.min^{0,5})**		
			10min	**20min**	**30min**	**72h**	**$C_{abs}N._{0\text{-}20min}$**	**$C_{abs}N._{20\text{-}30min}$**	**$C_{abs}N._{6\text{-}72h}$**
BR	0,55	0,16	1,07	1,12	1,17	2,64	0,266	0,058	0,019
BCNTs		0,2	0,98	1,06	1,13	2,34	0,251	0,064	0,016

III. Carbonation resistance

The main results of the carbonation test are presented in Table 8 for the uncracked concrete and in Table 9 and Table 10 for artificial and natural crack, respectively. Namely the carbonation depth (X_c), the carbonation depth in the crack area (X_F), the carbonation coefficient for the uncracked area (K_c) and the carbonation coefficient for the cracked area ($K_{C,F}$). In general, a good correlation with the square root of time was found (R^2>0.9). This confirms the suitability of Eq. (1), based on Fick's first law, in describing the carbonation depth evolution when steady hygrothermal conditions are maintained. In general, effective differences between compositions with and without CNTs were obtained, indicating that CNTs can improve the concrete resistance. Due to the drying process and preconditioning of the specimens, all mechanisms are likely involved in the reinforcement of the concrete matrix (filler, nucleation and bridging effect). Bridging can contribute to the reduction of the pore connectivity and consequently to CO_2 diffusion in concrete by retaining crack propagation and reducing crack width. The nucleation effect should improve the carbonation resistance by improving the microstructure of concrete and by increasing the amount of carbonated substances in the matrix.

As for the capillary absorption test in artificially cracked specimens, it was not possible to guaranty the same crack lengths in different concretes. Therefore, a new methodology was implemented to allow the comparison between compositions, regardless of the L_c. To this end, the carbonation coefficient through the crack ($K_{c,F}$) was determined by assuming that for carbonation depths higher than L_c, the carbonation front progresses at the same rate of that found in the current uncracked zone. Based on this assumption and taking into account Eq. (1), it is possible to estimate the time taken by the carbonation front to reach L_c (t_c) according to Eq. (6), where td is the total duration of the test (28 days) and $x_{c,28d}$ is the carbonation depth at 28 days. Finally, $K_{c,F}$ can be estimated form Eq. (7). Like the uncracked specimens, the artificially cracked ones, demonstrate a better behaviour when reinforced with CNTs. However, this improvement (10%) was lower than what was achieved in uncracked ones (18%). The carbonation depth, in cracked specimens, was significatively higher than expected and there was no obvious justification for it. One can only conclude that the crack concrete has worst quality. These specimens also presented similar values of carbonation depth in the cracked area. Also, the carbonation coefficients were basically the same. This means that CNTs had small or no contribution in this area of the specimen.

$$t_f = \left(\sqrt{t_d} - \frac{x_{c,28d} - L_f}{K_{c,zc}}\right)^2 \quad [6]$$

$$K_{c,F} = \frac{L_f}{\sqrt{t_f}} \quad [7]$$

Table 8 – Carbonation resistance (uncracked)

Mix.	w/c	X_c(mm)			K_c (mm/ano$^{0.5}$)	Δ(%)	R^2
		28d	56d	90d			
BR	0,55	7,0	10,2	12,7	25,7	-	0,99
BCNTs		5,6	9,1	9,9	21,1	17,9	0,98

In case of natural cracked specimens, the carbonation depth was lower than the crack depth, which allowed a direct calculation of the carbon coefficient in the cracked area. For this kind of cracks, it was only registered the carbonation depth at 7 and 28 days. Carbonation depth, respective coefficient and crack opening are presented in the Table 10. The carbonation rate was significatively higher in the cracked area and there was an influence of the crack width in the carbonation depth. For this case there was also a slight contribution of CNTs in mitigating the carbonation front, Therefore, it can be concluded that the induction of tortuous and rugged natural cracks, which promotes the bridging effect, led to lower carbonation rates than artificial cracks of equivalent width. Also note that induced cracks from bending tests are usually V-shaped, being narrower in depth.

Table 9 – Carbonation resistance for artificial cracks

Artificial crack														
Mistura	a/c	Lf	Uncracked area						Cracked area					
			X_c (mm)			$K_{c,ZC}$ (mm/ano$^{0.5}$)	Δ(%)	R^2	X_F (mm)			$K_{c,F}$ (mm/ano$^{0.5}$)	Δ(%)	
			28d	56d	90d				28d	56d	90d			
BR	0,55	18	10,2	12,4	14,5	31,2	-	0,97	17,2	19,3	23,2	67,1	-	
BCNTs		18	9,9	11,5	12,4	28,2	9,6	0,93	16,9	18,4	19,9	65,8	1,9	

Table 10 - Carbonation resistance for natural cracks

Natural crack													
Mistura	a/c	w_f	Uncracked area					Cracked area					
			X_c (mm)		$K_{c,ZC}$ (mm/ano$^{0.5}$)	Δ(%)	R^2	X_F (mm)		$K_{c,F}$ (mm/ano$^{0.5}$)	Δ(%)	R^2	
			7d	28d				7d	28d				
BR	0,55	0,06	2,9	7,3	25,1	-	0,98	10,2	19,9	72,3	-	0,99	
BCNTs		0,09	2,5	6,9	23,6	6,0	0,97	9,1	18,2	65,6	9,3	1	
BR		0,19	3,8	7,1	25,9	-	0,99	13,0	21,4	80,7	-	0,98	
BCNTs		0,17	3,5	7,1	25,5	1,5	0,99	10,2	20,5	73,9	8,4	1	

IV. Chloride penetration

The chloride penetration coefficient, crack depth and length are presented in the Table 11. CNTs had a modest contribution reducing the chloride penetration. Similar results, of about 7% reductions, where reported by other authors [13]. The chloride penetration test was carried out in water-cured conditions until testing, which prevented the development of shrinkage cracking. Moreover, contrary to the carbonation and capillary absorption tests, ion diffusion occurred through the specimen's thickness, further offsetting the possible effect of the CNTs upon arrest of surface microcracking. Therefore, chloride penetration resistance of uncracked specimens is not expected to take significant advantage of the bridging effect provided by CNTs. The eventual contribution of CNTs should in this case be limited to the filler and nucleation effects.

Table 11 - Chloride penetration resistance

		L_f	W_f	D_{cl}	Δ(%)
Uncracked	BR	-	-	15,81	-
	BCNTs	-	-	14,74	6,8
Artificial crack (0,05mm)	BR	20,1	0,05	15,70	-
	BCNTs	18,8	0,05	14,86	5,4
Natural crack (0,05mm)	BR	49,3	0,11	58,53	-
	BCNTs	48,5	0,07	37,17	36,5
Natural crack (0,1mm)	BR	49,4	0,16	66,44	-
	BCNTs	48,6	0,18	43,07	35,2

Fig. 7 shows the test results for the artificially cracked concrete. Indicating a substantial rise of the chloride coefficient in the cracked area, up to 70% higher than what was registered in the uncracked area. CNTs were able to reduce this with only 58% difference between the two areas. It's important to notice that in artificially cracked specimens, it is not only the

cracked area that is affected by the chloride penetration, the surrounding area also suffers from it, as it is shown in Fig. 8.

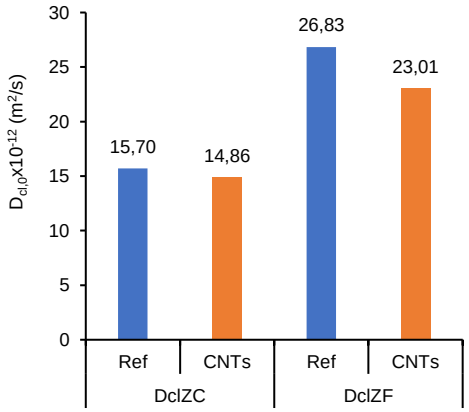

Fig. 7 – Chloride coefficients in artificial cracked specimens

There was a substantial rise in the D_{cl} on the natural cracked specimens. This was mainly because of the different size and geometry of this specimens. In addition, the crack goes through all the thickness of the specimens which speeds up the chloride penetration. Comparing the results of the two concrete mixes it is possible to identify a higher contribution of CNTs in the uncracked area, with a reduction of about 35% in the D_{cl}. Such results can be justify by 3 main reason: The uncracked area is also affected by the crack; the best contribution of CNTs is next to the crack area, due to the cracking method, which promoted the appearance of microcracking and therefore promoted bridging mechanisms; different crack widths with reinforced concrete having smaller cracks. CNTs had lower contributions in the crack chloride coefficient. As reported, the crack is too large for the CNTs to work and the bridging effect is less relevant.

Fig. 8 – Specimens subject to chloride attack

4. Conclusion

In this study, the durability of cracked concrete reinforced with CNTs was analysed. The tests performed were capillary absorption, carbonation and chloride penetration behaviour. The following main conclusions have been drawn:

- The workability and density of concrete was little affected by the addition of 0.1%wtc CNTs. This was attributed to the good dispersion of CNTs attained with appropriate dispersants, which did not significantly affect the air content of concrete.
- Improvements up to 10 % were registered in the mechanical properties of the reinforced concrete. These were modest improvements which proved that filler, nucleation and bridging effect happened inside the concrete matrix. Difficulties in the dispersion of the CNTs may justify such results. The CNTs used in the present study could also have poor quality, since they were stored for a long time.
- Capillary absorption was lower in reinforced concretes. This shows that CNTs contributed for the refinement of the concrete matrix by nucleation and filler effect. This improvement was more relevant in later stages of the capillary absorption test.
- Cracked specimens had higher absorption than uncracked ones and the crack width had influence in the water absorption. For similar crack openings, natural cracks had better results, this was because of the crack behaviour which is tortuous and has v shaped format.
- The Carbonation resistance was up to 18% lower in reinforced concrete. Nucleation and filler effect contributed to the refinement of the concrete microstructure. The long drying process and pre-conditioning method allowed microcracking which promoted bridging.
- Normal and reinforced concrete had little to none differences in the carbonation coefficient of the crack area for the artificial cracked specimens. In the other hand, natural cracks revealed an improvement of the same coefficient for the reinforced concrete. This shows that the natural crack promotes the contribution of CNTs by bridging mechanisms.
- For the Chloride resistance, in reinforced concrete, modest improvements were registered. The low level of microcracking in the concrete translates that only nucleation and filler effect are working inside the concrete.
- In natural cracked specimens the chloride resistance was up to 35% better in reinforced concrete. This was mainly because of the cracking method which promoted microcracking and therefore the activation of bridging.
- In general, CNTs work in a effective way in the improvement of the concrete resistance. Whenever microcracking was present this improvement was more noticeable.

References

[1] Yu, M., Lourie, O., Dyer, M. J., Moloini, K., Kelly, T. F., & S., R. R. (2000). Strength and Breaking Mechanism of Multiwalled Carbon Nanotubes Under Tensile Load. Science, 287(5453), 637–640.

[2] Gao, L., Jiang, L., & Sun, J. (2006). Carbon nanotube-ceramic composites. Journal of Electroceramics, 17(1), 51–55.

[3] Samal, S. S., & Bal, S. (2008). Carbon Nanotube Reinforced Ceramic Matrix Composites- A Review. Journal of Minerals and Materials Characterization and Engineering, 7(4), 355.

[4] S. Mindess, J. Young, D. Darwin (2003). Concrete, second ed., Prentice Hall, Pearson Education.

[5] P. Mehta, P. Monteiro (2006). Concrete: Microstructure, Properties and Materials, McGraw-Hill Professional Publishing.

[6] T. Nochaiya, A. Chaipanich (2011). Behavior of multi-walled carbon nanotubes on the porosity and microstructure of cement-based materials, Appl. Surf. Sci. 257 (6), 1941–1945.

[7] M. Guedes, H.H. Ahmed, J.A. Bogas, S. Olhero (2016). Experimental Procedure for Evaluation of CNT dispersion in High pH Media Characteristic of Cementitious Matrixes, in: Livro Atas Do 1o Congr. Ensaios E Exp. Em Eng. Civ. – TEST&E 2016, Instituto Superior Técnico, Lisboa-Portugal.

[8] R.K. Abu Al-Rub, A.I. Ashour, B.M. Tyson (2012). On the aspect ratio effect of multiwalled carbon nanotube reinforcements on the mechanical properties of cementitious nanocomposites, Constr. Build. Mater. 35, 647–655,

[9] M.S. Konsta-Gdoutos, Z.S. Metaxa, S.P. Shah (2010). Highly dispersed carbon nanotube reinforced cement based materials, Cem. Concr. Res. 40, 1052–1059,

[10] EN 12350-2: 2009. Testing fresh concrete. Slump test. CEN.

[11] EN 12390-3: 2009. Testing hardened concrete. Compressive strength of test specimens. CEN,

[12] LNEC E391: 1993. Concrete. Carbonation resistance. LNEC, Lisbon.

[13] Carriço A, Bogas JA, Hawreen A, Guedes M. (2018). Durability of multi-walled carbon nanotube reinforced concrete. Construction and Building Materials, 164, 121-133.

[14] LNEC E393: 1993. Concrete. Capillary absorption. LNEC, Lisbon.

[15] NTBUILD 492 (1999). Concrete mortar and cement-based repair materials: chloride migration coefficient from non-steady-state migration experiences. Nordtest.

[16] J. Makar, J. Margeson, J. Luh (2005). Carbon Nanotube/Cement Composites – Early Results and Potential Applications, in: 3rd Int. Conf. Constr. Mater. Performance, Innov. Struct. Implic.1–10.

[17] R.K.A. Al-Rub, B.M. Tyson, A. Yazdanbakhsh, Z. Grasley (2012). Mechanical properties of nanocomposite cement incorporating surface-treated and untreated carbon nanotubes and carbon nanofibers, J. Nanomech. Micromech. 1 3–8.

[18] F. Collins, J. Lambert, W.H. Duan (2012). The influences of admixtures on the dispersion, workability, and strength of carbon nanotube – OPC paste mixtures, Cem. Concr. Compos. 34, 201–207.

[19] M.S. Konsta-Gdoutos, Z.S. Metaxa, S.P. Shah (2010). Highly dispersed carbon nanotube reinforced cement based materials, Cem. Concr. Res. 40, 1052–1059,

[20] Hawreen A, Bogas JA, Kurda R. (2019). Mechanical characterization of concrete reinforced with different types of carbon nanotubes. Arabian Journal for Science and Engineering, 44, 8361–8376.